Journal of Theoretical and Applied Mechanics, Sofia, Vol.54 (2024) pp. 61-72
SOLID MECHANICS

MICROSTRUCTURAL ANALYSIS OF 40X STEEL AFTER STRAIN-CONTROLLED FATIGUE

VANYA DYAKOVA[1*], YANA MOURDJEVA[1], TATIANA SIMEONOVA[1,2], RUMEN KRASTEV[2], ILIAN ATANASOV[1], LUDMIL DRENCHEV[1], VASIL KAVARDJIKOV[2]

[1]*Institute of Metal Science, Equipment and Technologies, Acad. A. Balevski Hydro- and Aerodynamics Centre, Bulgarian Academy of Sciences, Sofia, Bulgaria*
[2]*Institute of Mechanics, Bulgarian Academy of Sciences, Sofia, Bulgaria*

[Received: 25 July 2022. Accepted: 9 March 2023]

doi: https://doi.org/10.55787/jtams.24.54.1.061

ABSTRACT: Specimens of 40X steel were tested in tension and strain controlled low-cycle fatigue. It was found that the increase of strain amplitude leads to a decrease in the exploitation durability of 40X steel. The microstructure evaluation after cyclic tests with 0.18% and 0.35% deformation amplitude was investigated. The existing in the initial materials state banding in the rolling direction is preserved after cycling loading, but with increase of deformation amplitude, ferrite is refined, cementite lamellae break and spheroidal cementite is aggregated. Dislocation substructure also changes – dislocation walls are compacted, dislocation network develops, dislocation tangles appear. New dislocation walls are formed from parallel screw dislocations with the same sign. The state is characteristic of volumes with high level of elastic deformation.

KEY WORDS: 40X steel, strain controlled low-cycle fatigue, microstructure.

1 INTRODUCTION

Fatigue is a progressively developing, localized structural change that occurs in a metal under multiple or fluctuating deformations at nominal stresses that have maximum values less than the proof strength of the material. Fatigue can culminate in cracks and cause breakage after a sufficient number of fluctuations.

Fatigue damage is exhibited in microstructural changes as a consequence of cyclic elasto-plastic deformation. It is known that near the threshold region the development and growth of fatigue cracks are greatly influenced by the microstructural el-

*Corresponding author e-mail: v_diakova@ims.bas.bg

ements of the metal such as grain size, volume fraction of the second phase, inclusions, etc. [1–7]. There is insufficient information in the literature on microstructural changes during fatigue loading and investigation of its influence on fatigue crack growth resistance.

It was found that the morphology of the solid phase has influence on the growth of fatigue cracks in low carbon steel [6]. The fatigue crack growth behavior of two different two-phase steels with a ferrite-martensite microstructure – AISI 1018 and Fe2Si0.1C [7] was studied: the microstructure of one steel is a continuous ferrite matrix with encapsulated islands of martensite (a continuous ferrite matrix with islands of martensite encapsulated (FEM), and of the other – a continuous martensite with islands of ferrite encapsulated (MEF). It was found that the microstructure of MEF has a higher yield strength and resistance to fatigue crack growth than that in the FEM microstructure It has been shown in [8] that the solid phase can deflect the crack growth path.

The effect of pearlite morphology on fatigue crack growth behavior was investigated in [9]. Both randomly distributed and networked pearlite structures were considered in this study. It was found that in the Paris mode, the resistance to fatigue crack growth in steel with distributed pearlitic structure was higher than that of steel with network pearlitic structure.

Structural steels are usually used for the manufacturing of high strength elements – axles, shafts, gears, pistons, rods, crankshafts and camshafts, rings, spindles, mandrels, rails, spongy rims, bolts, half-axles, bushings and other elements [10]. During operation, such elements are often subjected to cyclic loading, which is accompanied by elastic and plastic deformation, leads to material fatigue, crack formation and failure.

In elastic distortions of the metal lattice, the possibility of simultaneous development of several processes in the dislocation structure appears: changes in the internal structure of the dislocation walls and the formation of segregations of alloying or impurity elements on them [11].

During plastic deformation, the evolution of the microstructure of metals manifests itself in additional enrichment with dislocations, annihilation and rearrangement, and shear band formation [12]. A number of studies on the relationship between macroscopic plastic deformation and changes in dislocation structures have been reported [13–16]. These studies show that dislocation structures and their evolution during deformational cyclic loading mainly depend on the plastic deformation amplitude.

Studying the relationships between low-cycle fatigue performance and the microstructure of steels leads to a better understanding of the fatigue process of the material preceding crack formation and failure.

2 Experimental Part

2.1 Material

Material used in current investigation is 40X steel with chemical composition presented in Table 1.

Table 1: Chemical composition of 40X steel, mass.%

C	Si	Mn	Ni	S	P	Cr	Cu
0.36–0.44	0.17–0.37	0.5–0.8	< 0.3	< 0.035	< 0.035	0.8–1.1	< 0.3

Uniform-gage specimens with a solid circular cross section and straight sided collet-grip are used for both tensile and fatigue tests. Specimens' dimensions are as follows: 8 mm diameter and 30 mm length of a test section, 10 mm diameter of a collet-grip and total specimen length of 130 mm. The roughness of the working surface of the sample is Rz $= 6.3$ μm. The test specimens are not heat treated.

2.2 Mechanical characterization

Mechanical tests were performed on a Zwick-Roell HA-250 servo-hydraulic testing machine. The strain was measured with a Sandner EXA 25-2.5o extensometer with a 25 mm base length.

Tensile properties are determined at room temperature according to ISO 6892-1.

Fatigue tests were performed according to the ASTM 606/E606M [17]. Cyclic sinusoidal strain amplitudes (tension-compression) in the range of 0.18% to 0.60% with mean strain being 0% at the start of each test were used. The variation of the stress amplitude over time and the number of cycles until the failure of the specimen are controlled. The separation of the strain measured at one cycle into elastic and plastic is described in the standard. The software calculates the plastic deformation for each cycle and its evolution during the test. The tests were carried out in a temperature chamber at 25°C.

2.3 Microstructural characterization

The microstructure of the material was investigated by the methods of light (LM) and transmission electron microscopy (TEM).

Specimen No 1 was observed in the initial material state. Specimens No 2 and No 3 were observed after the fatigue tests with deformation amplitudes of 0.18% and 0.35%, respectively. The specimen No 2 has withstood 500000 cycles without failure and the specimen No 3 – 15900 cycles before breaking.

The metallographic samples for LM are prepared according to a standard procedure by grinding, polishing and etching of pieces cut longitudinal to the rolling direction (RD) and fatigue loading direction (FLD) of the test specimens No 1, No 2 and No 3. The observation was performed with Zeiss light microscope with a digital camera.

TEM observations are made on carbon replicas and metal foils. The observation plane of carbon replicas, like metallographic samples, is parallel to the steel rolling direction and to the fatigue load direction. The plain of the observation of the foils is perpendicular (cross section) of rolling and fatigue direction. The cut discs with 3 mm were thinned to a thickness of 25–30 μm, and were polished electrochemically. The observations were performed with a transmission electron microscope JEOL-JEM 1011 proceeding at 100 kV accelerating voltage.

3 Results and Discussion

The results for the mechanical characteristics of the studied material are presented in brief, only as they are needed for studying the relationship between fatigue test parameters and microstructural changes. More details of the conducted static and cyclic tests are described in [18].

3.1 Tensile properties

Mechanical properties of steel 40X obtained from the static tensile tests are presented in Table 2.

Table 2: Tensile test results of steel 40X

Elastic modulus E [GPa]	Proof strength $R_{p0.2}$ [MPa]	Tensile strength R_m [MPa]	Elongation at break A_t [%]	Reduction of area Z [%]
195 ± 5	649 ± 11	809 ± 12	15.8 ± 0.5	51 ± 2

3.2 Development of the plastic strain

Standard ASTM E606M [2] describes a mathematical apparatus for interpreting results from strain-controlled fatigue tests

$$\frac{\Delta\varepsilon}{2} = \frac{\Delta\sigma}{2E} + \frac{\Delta\varepsilon_p}{2}\,, \tag{1}$$

where the total axial strain for a cycle loop is $\Delta\varepsilon$, $\Delta\sigma/2$ is the stress amplitude, E is the elastic modulus and $\Delta\varepsilon_p$ is the plastic strain for the whole cycle. The soft-

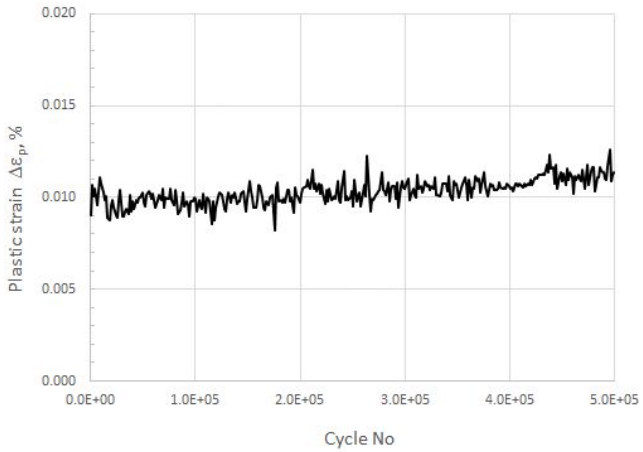


Fig. 1: Development of plastic strain for a test with 0.18% strain amplitude.

ware determines elastic modulus for each cycle and calculates the plastic strain in millimeters using Eq. (2)

$$\Delta\varepsilon_p = \Delta\varepsilon - \frac{\Delta\sigma}{E}\,. \tag{2}$$

Figure 1 shows non-elastic deformation obtained by Eq. (2) at 0.18% total strain amplitude. This specimen endured 500 000 cycles and the test was stopped without fracture.

Development of the plastic deformation for a specimen tested with 0.35% strain amplitude is shown in Fig. 2. The diagram typically can be divided into three stages –

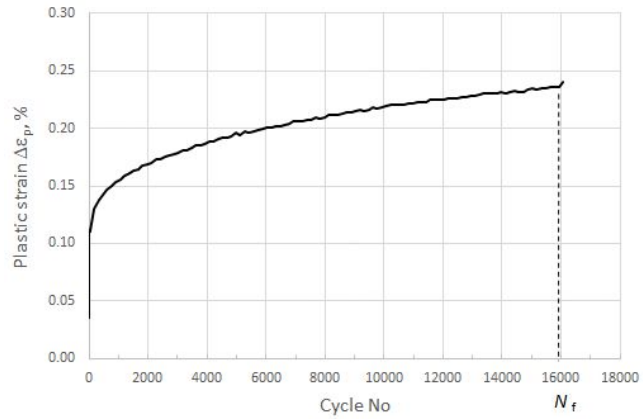


Fig. 2: Development of plastic strain at 0.35% strain amplitude.

fast-growing in the beginning, steady growing and catastrophic failure with sudden rise of the measured plastic strain curve. In case with Fig. 2 the number of the cycles till failure is determined to be 15900 and this is the moment when plastic strain increases due to the rapid development of fatigue crack, leading to fracture of the tested sample.

Table 3 shows results for the fatigue behavior of 40X steel specimens, selected for microstructural analysis. It can be seen that lower loads generate lower plastic strains. From experimental results it can be concluded that the increasing in plastic strain leads to some relaxation and decrease in stress amplitude during the experiment.

Table 3: Fatigue test results of 40X steel specimens

Specimen designation	$\varepsilon_{\max}$ %	$\Delta\sigma/2$ [MPa] at test beginning	$\Delta\sigma/2$ [MPa] at test end	$\Delta\varepsilon_p$ [%] at test end	Number of cycles	Test duration [min]
No 2	0.18	319	318	0.011	> 500000	417
No 3	0.35	506	385	0.236	15900	20.6

3.3 LOW-CYCLE FATIGUE

In order to present the low-cycle fatigue behaviour to failure of 40X steel a failure criterion is accepted, which correspond to the moment when the measured "plastic strain" starts to grow fast, because of the development of a crack inside the measured base length. The resulting diagram of cycles to failure depending on the strain amplitude is shown in Fig. 3.

The curve named "Empiric" is an approximation of experimental data done by power function (eq. (3))

$$\frac{\Delta\varepsilon}{2} = 0.0275\, N_f^{-0.213}\,, \tag{3}$$

where $\Delta\varepsilon/2$ is the strain amplitude (dimensionless) and N_f is the number of cycles to failure. The same data is approximated theoretically using eq. (4) from ASTME606M standard and its graph is named "Curve"

$$\frac{\Delta\varepsilon}{2} = \frac{\sigma'_f}{E}\,(2N_f)^b + \varepsilon'_f\,(2N_f)^c\,. \tag{4}$$

Where fatigue strength exponent $b = -0.031$, fatigue ductility exponent $c = -0.787$, fatigue strength coefficient $\sigma'_f = 557$ MPa, fatigue ductility coefficient (dimensionless) $\varepsilon'_f = 2.59$ and Young's modulus $E = 181$ GPa.

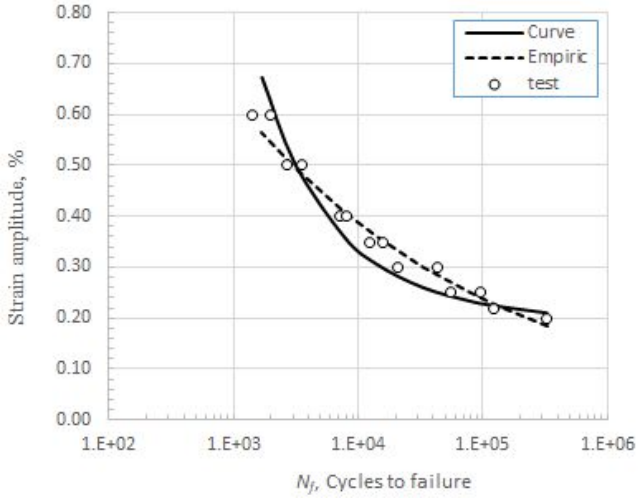


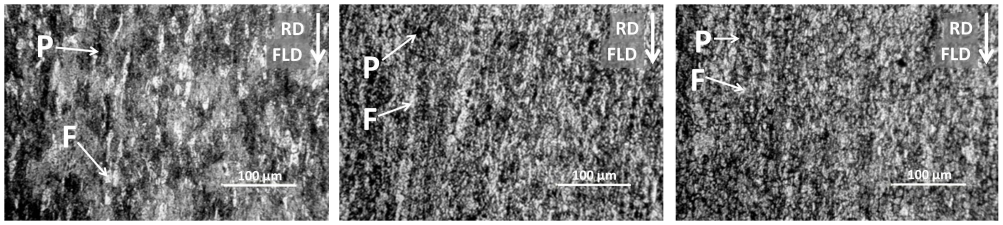
Fig. 3: Low-cycle fatigue behaviour to failure of 40X steel, according to the strain amplitude.

3.4 MICROSTRUCTURAL CHARACTERIZATIONS

The microstructure of 40X steel is ferrite-pearlitic (Figs.4–6). The white areas on the photos are ferrite and the dark ones are perlite.

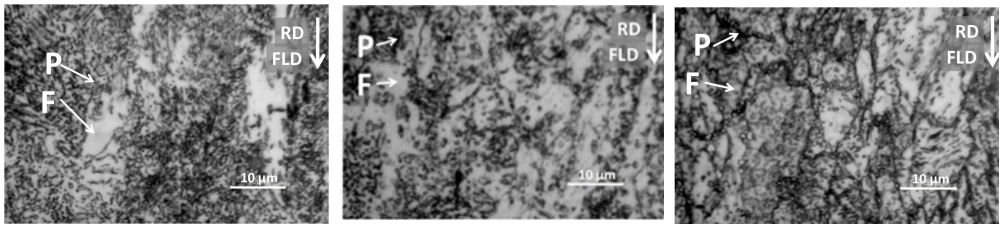
clear orientation in the rolling direction is observed (Fig. 4(a)) of the 40X steel microstructure before the fatigue test (Specimen No 1). The ferrite grains are elongated to (40÷45) μm and wide up (7÷8) μm (Fig. 6(a)). Both types perlite – spheroidal and lamellar – are observed. The spheroidal pearlite is with rounded cementite plates with a diameter up to (0.2÷0.3) μm and lamellar pearlite is with the length of the cementite lamellae up to (1.2÷1.4) μm.

After the fatigue tests, the steel microstructure orientation in the rolling directions preserved, but the ferrite grains refined. (Figs. 4(b), 4(c)). As the deformation



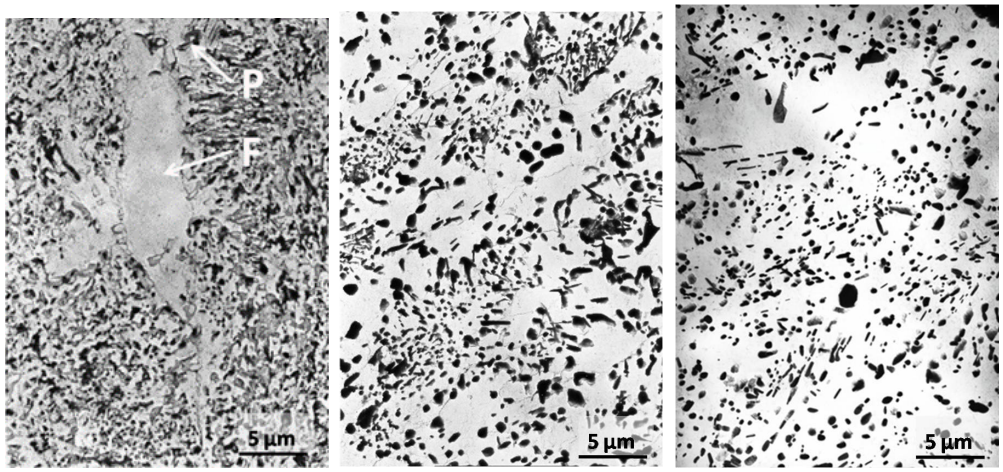
(a) Specimen No 1 (b) Specimen No 2 (c) Specimen No 3

Fig. 4: Microstructure of the tested specimens, LM.



(a) Specimen No 1 (b) Specimen No 2 (c) Specimen No 3

Fig. 5: Microstructure of the tested specimens, LM.

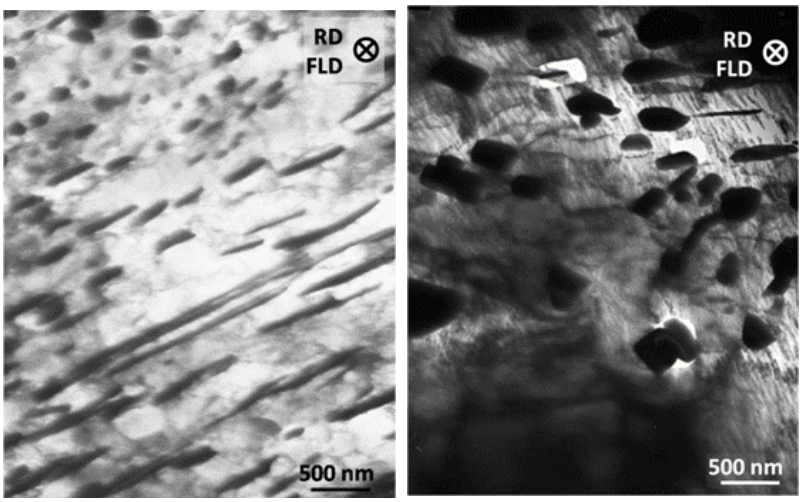


(a) Specimen No 1 (b) Specimen No 2 (c) Specimen No 3

Fig. 6: Microstructure of the tested specimens, replicas.

amplitude increases to 0.35%, the ferrite grains lose their clearly defined boundaries (Figs. 5(b), 5(c)). Pearlite "penetrates" the ferrite. The cementite lamellae are fractured and the spheroidal cementite aggregates to 0.5 μm in diameter (Figs. 6(b), 6(c), 7(a), 7(b)).

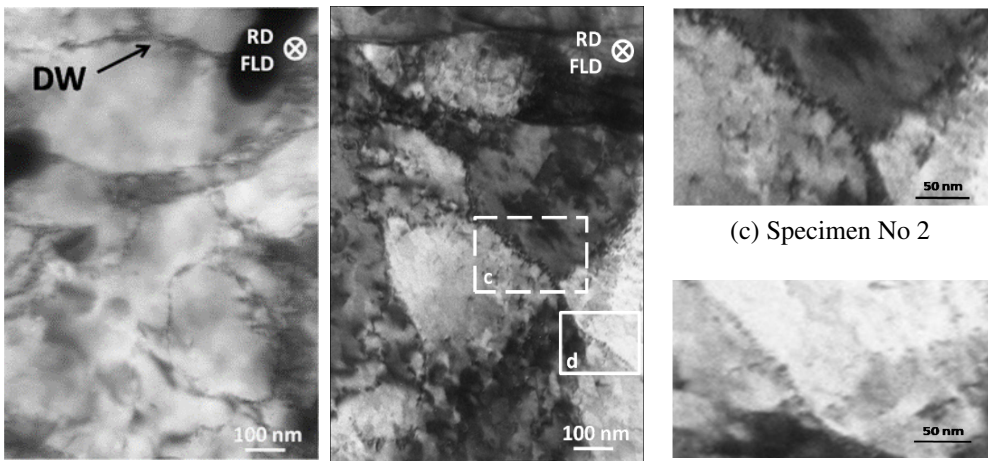
TEM images of metal foils show changes of the steel dislocation structure due to fatigue tests. A well-formed dislocation network is observed in the undeformed specimen No 1. Dislocation cells have clearly defined dislocation walls, single dislocations are absent in them (Fig. 8(a)). As the deformation amplitude increases, the dislocation walls are compacted, single dislocations appear in the cells, their density gradually increases, dislocation networks and dislocation tangles are formed (Fig. 8(b)).



(a) Specimen No 1 (b) Specimen No 2

Fig. 7: Microstructure of the tested specimens (cross section), TEM – folio.

The formation and evolution of the dislocation substructure during deformation occurs through limited repeated sliding and annihilation of individual mobile dislocations under the influence of elastic interaction forces, as a result walls of parallel dislocations with the same sign are formed in separate planes [19–21]. Under such



(a) Specimen No 1 (b) Specimen No 2 (c) Specimen No 2 (b) Specimen No 2

Fig. 8: Dislocation configurations in the observed specimens, TEM – folio.

conditions, first of all, group-parallel screw dislocations are formed, which have the highest mobility according to the specified mechanism, due to the absence of strictly defined sliding planes in them. The indicated process has a significantly lower speed at edge dislocations due to the need of limited development of the creep process. The main characteristics of the individual wall consisting of parallel screw dislocations are a high level of elastic deformations in the surrounding volumes of the crystal and their extremely high mechanical instability [20].

Due to deformation, zones with an increased concentration of impurity atoms - the so-called Cottrell atmosphere – are formed around the dislocation lines as a result of the interaction of the elastic stress field of the dislocations and impurity atoms of embedding. In steels in these zones, the most strongly attracted by dislocations are carbon and nitrogen atoms. Penetrating the ferrite, the carbon atoms connect with the iron atoms and cementite is released in the form of lamellae with a length of 5÷20 nm. The cementite lamellae are both parallel to the screw dislocations and to each other and are visible in Figs. 8(b), (c), (d). There is ferrite between the lamellae, which together with cementite lamellae forms a very narrow band of pearlite. This process also occurs with single cementite inclusions located around the dislocations within the ferrite subgrains. In this way, the pearlite "penetrates" the ferrite, which was found in the observation by LM and TEM (Figs. 5(b), 5(c), 6(b), 6(c)).

4 Conclusions

The fatigue strength of 40X steel was determined following standard ASTM E606/ E606M for strain-controlled fatigue tests. As expected, the increase of the strain amplitude leads to a decrease in the exploitation durability of 40X steel. The fatigue under 0.35% strain amplitude leads to rapid development of plastic strain up to 0.236% and fracture of the sample after 16×10^3 cycles. The lower deformation amplitude of 0.18% generates insignificant plastic strain in investigated material which is kept almost constant till 5×10^5 cycles without fracture.

It was found that after the fatigue tests at deformation amplitudes of 0.18% and 0.35%, the microstructure of steel 40X preserves the initial directionality of the rolling and loading directions, but the ferrite grains are refined, the cementite lamellae are broken, and the spheroidal cementite is aggregated to 0.5 μm in diameter. The pearlite "penetrates" the ferrite.

The dislocation structure also changes – a network of dislocation cells with compacted walls is developed, dislocation walls are formed from parallel screw dislocations with the same sign, which is characteristic for volumes with high level of elastic deformation and high mechanical instability.

ACKNOWLEDGMENTS

This report is a research result of project BG05M2OP001-1.001-0008 "National Center for Mechatronics and Clean Technologies", funded by the Operational Program "Science and Education for Smart Growth" 2014-2020, co-financed by the European Union through the European Fund for Regional Development.

REFERENCES

[1] D. TAYLOR (1984) Analysis of data on fatigue crack propagation thresholds.

[2] Y. MUTOH, V.M. RADHAKRISHNAN (1986) Effect of yield stress and grain size on threshold and fatigue limit. *Journal of Engineering Materials and Technology* **108**(2) 174-178.

[3] R. PIPPAN (1991) Threshold and effective threshold of fatigue crack propagation in ARMCO iron. I. The influence of grain size and cold working. *Materials Science and Engineering: A* **138**(1) 1-13.

[4] S. TAIRA, K. TANAKA, M. HOSHINA (1979) Grain size effect on crack nucleation and growth in long-life fatigue of low carbon steel. In: J. Long (ed) "Fatigue Mechanisms", ASTM STP 675-EB, pp. 135-173.

[5] J.C. RADON, J. WOODTLI (1984) Influence of microstructure on the cyclic crack growth in a low-alloy steel. *International Journal of Fatigue* **6**(4) 221-227.

[6] J.A. WASYNCZUK, R.O. RITCHIE, G. THOMAS (1984) Effects of microstructure on fatigue crack growth in duplex ferrite-martensite steels. https://doi.org/10.1016/0025-5416(84)90269-6*Materials Science and Engineering* **62**(1) 79-92.

[7] H. SUZUKI, A.J. MCEVILY (1979) Microstructural effects on fatigue crack growth in a low carbon steel. https://doi.org/10.1007/BF02697075*Metallurgical Transactions A* **10** 475-481

[8] K. MINAKAWA, Y. MATSUO, A.J. MCEVILY (1982) Influence of a duplex microstructure in steels on fatigue crack growth in the near-threshold region. *Metallurgical Transactions A* **13** 439-445.

[9] A.A. KORDA, Y. MIYASHITA, Y. MUTOH, T. SADASUE (2007) Fatigue crack growth behavior in ferritic–pearlitic steels with networked and distributed pearlite structures. *International Journal of Fatigue* **29**(6) 1140-1148.

[10] N.V. THIEN, D.H. TIEN, N.T. NGUYENA, N.V. QUE, D.D. TRUNG, P.T. THOA (2020) A prediction of Cutting Force, System Vibration, and Productivity in Five-Axis Milling Process of the Spiral Bevel Gear. *Advances in Science, Technology and Engineering Systems Journal* **5**(6) 1394-1401.

[11] I.F. TKACHENKO, .. KACHENKO, V.. IROSHNICHENKO (2016) Some features of the heterogeneous diffusive nucleation and their use to form new type microstructures and eliminate chemical nonuniformities in bulk industrial product made of alloy structural steels. Ukraine Svidotstvo No 68323 dated 25.10.2016. Application No 68903 dated 25.08.2016, Ukraine.

[12] M.S. PHALM, S.R. HOLDSWORTH, K.G.F. JANSSENS, E. MAZZA (2013) Cyclic deformation response of AISI 316L at room temperature: mechanical behavior, microstructural evolution, physically-based evolutionary constitutive modelling. *International Journal of Plasticity* **47** 143-164.

[13] Y. LI, C. LAIRD (1994) Cyclic response and dislocation structures of AISI 316L stainless steel. Part 1: single crystals fatigued at intermediate strain amplitude. *Materials Science and Engineering: A* **186**(1-2) 65-86.

[14] T. MAYAMA, K. SASAKI, M. KURODA (2008) Quantitative evaluations for strain amplitude dependent organization of dislocation structures due to cyclic plasticity in austenitic stainless steel 316l. *Acta Materialia* **56**(12) 2735-2743.

[15] S.G. HONG, S.B. LEE (2004) The tensile and low-cycle fatigue behavior of cold worked 316L stainless steel: Influence of dynamic strain aging. *International Journal of Fatigue* **26**(8) 899-910.

[16] D. YE, S. MATSUOKA, N. NAGASHIMA, N. SUZUKI (2006) The low-cycle fatigue, deformation and final fracture behaviour of an austenitic stainless steel. *Materials Science and Engineering: A* **415**(1-2) 104-117.

[17] ASTM E606/606M-12 Standard Test Method for Strain-Controlled Fatigue Testing.

[18] R. KRASTEV, T. SIMEONOVA, V. KAVARDJIKOV, I. ATANASOV, L. DRENCHEV (2022) Strain controlled fatigue of 40X steel. *International Scientific Journal Machines. Technologies. Materials.* **16**(4) 146-149.

[19] J.W. CHRISTIAN (1975) "The theory of transformations in metals and alloys. Part 1". Pergamon Press, London, England.

[20] R. SEDLÁČEK, W. BLUM, J. KRATOCHVL, S. FOREST (2002) Subgrain formation during deformation: physical origin and consequences. *Metallurgical and Materials Transactions A* **33** 319-327.

[21] I.F. TKACHENKO, F.K. TKACHENKO, K.I. TKACHENKO, V.I. MIROSHNICHENKO (2016) Influence of the equilibrium dislocation substructure on the structure component morphology in the heterogeneous phase transformations in polycrystalline metallic alloy. *Reporter of the Priazovskyi state technical university. Section: Technical sciences* **33**(1) 50-57.